Gas Processing Journal
Vol. 10, No. 1, 2022, pp. 1 - 18
http://gpj.ui.ac.ir
Research Paper

Developing a new hydrogen liquefaction process through configuration modification and parameter optimization

Hamed Rezaie Azizabadi*[1], Masoud Ziabasharhagh[1], Mostafa Mafi[2],

[1] Faculty of Mechanical Engineering, K.N. Toosi University of Technology, Tehran, Iran
[2] Faculty of Mechanical Engineering, Imam Khomeini International University, Qazvin, Iran

Received: 2021-05-25 Revised: 2021-09-18 Accepted: 2021-12-01

Abstract: A new concept for hydrogen liquefaction with a capacity of 300 tons per day is developed through the modification of an existing one. Pressure and temperature levels, mixed-refrigerant composition, and different configurations are explored to achieve a new concept with lower SEC and higher COP. Aspen HYSYS V9 is used to simulate the process. Exergy and energy analyses are employed for evaluating the process to capture the effect of changes. As different parameters of the liquefaction process are interlinked and depend on each other, optimization is done using a trial and error procedure. Modified-Benedict–Webb–Rubin and Peng-Robinson equations of state are utilized to simulate hydrogen and mixed refrigerant streams to increase the accuracy of the results, especially for the ortho-para conversion. Power consumption of the coolers is considered, and exergy destruction for all the components is calculated. It is found that ortho-para converters and separators could affect the total exergy destruction and efficiency of the process; however, their exergy efficiency is nearly 100%. The SEC of the new concept is 5.97 kWhr/kg, which shows an 18.8% improvement compared to the base concept. The COP and ε are improved by 14.4% and 15.5% too. The results show that the liquefaction section is responsible for 85% of the total SEC of the process, and it deserves to focus on this section for future studies.

keywords: Hydrogen liquefaction, Exergy analysis, Aspen HYSYS, Mixed-refrigerant, Ortho-Para Conversion.

1. Introduction to hydrogen

Energy is a crucial subject since its significance for the economy, environment, and many vital aspects of human life have been proved. It is expected that the world's energy demands will be doubled compared to today's amounts by the year 2040. Problems caused by the harmful gaseous emissions are increasing, so the energy sectors need low-emission and low-carbon sources of energy [1]. Hydrogen is introduced as an alternative to old fuels since it liberates a considerable quantity of energy per unit weight without producing CO_2 [2]. Hydrogen is an abundant element, and it can be derived from sustainable and environmentally friendly resources, so it is expected to play a substantial role in the future. Using hydrogen is tangled with many challenges as it is the lightest material except helium. Hydrogen typically occupies a massive volume due to its low energy density [3]. The energy density of hydrogen can be enhanced by liquefaction; however, the boiling temperature of hydrogen is as low as 20 K, and nearly one-third of its energy contents areconsumed in the liquefaction process [1]. Until now, most of the constructed hydrogen liquefaction plants are similar to the first one established in the United States, with exergy efficiencies between 20%-30% [4]. It seems that optimization and development of new technologies for mass production of liquid hydrogen are indispensable for improving the hydrogen economy [5]. Hydrogen shows promising features; therefore, it could be the right fuel for the future if the involved challenges are conquered.

The first successful liquefaction of permanent gases is attributed to Cailletet L.'s in 1877 [6]. Sir James Dewar Scottish/British scientist in 1898,

* Corresponding Author.
Authors' Email Address: [1] H. Rezaie Azizabadi (h.rezaie@mail.kntu.ac.ir), [2] M. Ziabasharhagh (mzia@kntu.ac.ir), [3] M. Mafi (m.mafi@eng.ikiu.ac.ir)

2345-4172/ © 2022 The Authors. Published by University of Isfahan
This is an open access article under the CC BY-NC-ND/4.0/ License (https://creativecommons.org/licenses/by-nc-nd/4.0/).

http://dx.doi.org/ 10.22108/GPJ.2021.128850.1102

liquefied hydrogen with a flow rate of 4 cc/min using the Joule-Thompson effect [7]. Baker and Shaner [8] studied a large-scale liquefaction process with a capacity of 250 tons per day (TPD) and continuous ortho-para conversion. They used nitrogen and the Claude cycle for pre-cooling and liquefaction in turn. The exergy efficiency of the process has been reported as 36%. Matsuda and Nagami [9] introduced four different concepts for hydrogen liquefaction in the WE-NET[1] project, including a 300 TPD capacity with nitrogen pre-cooling. They show that the Claude cycle is the most appropriate process for hydrogen liquefaction. Quack [10] made a new large-scale concept with the capacity of 170 TPD and suggested dividing the hydrogen liquefaction process into four sub-processes, including; pre-compression, pre-cooling (ambient to 80 K), cryo-cooling (80 K to 30 K) and liquefaction (30 K to LH_2 at 1 bar).

Staate [11] proposed a supercritical cycle with helium as the refrigerant and high-pressure hydrogen feed. Yuksel et al. [1] presented a novel supercritical hydrogen liquefaction process with helium cooling. The energy and exergy efficiencies are reported as 70.12% and 57.13%, respectively. Valenti and Macchi [12] presented an innovative, large-scale concept with a mass flow rate of 10 kg/s. The exergy efficiency was reported as 47.73%. Berstad and Neska [13] proposed a new concept with mixed-refrigerant (MR) refrigeration and reversed helium-neon Brayton cycle as pre-cooling and liquefaction, respectively. They replaced expansion valves with liquid expanders to yield higher efficiency. Krasae-in et al. [14] simulated a 100 TPD hydrogen liquefaction plant with MR and Joule-Brayton cascade refrigeration as pre-cooling and liquefaction, respectively. Valenti et al. [15] studied the effect of thermodynamic modeling of the fluid on large-scale hydrogen liquefiers. They found that the process's accuracy is deeply affected by choice of a heat capacity model. Walnum et al. [16] divided the liquefaction process into four sub-processes and focused on the pre-cooling as it has the most degree of freedom. Krasae-in et al. [17] modified a novel 100 TPD concept with two MR refrigeration cycles for pre-cooling and four cascades Brayton refrigeration cycles for liquefaction. The modified plant has an overall power consumption of 5.91 kWh/kg_{LH_2}. Quack et al. [18] explored an optimum hydrogen liquefaction process with a mixture of helium and neon, called "Nelium". Results show that helium-rich mixtures can exchange heat better, while neon-rich mixtures have superior compression features. Turbo-expanders with higher efficiencies could be employed due to the presence of neon in the mixture. Asadnia et al. [19] proposed a novel MR configuration for liquefaction of hydrogen with a capacity of 100 TPD. They utilized a Joule-Brayton refrigeration cycle for cooling feed hydrogen from 25 °C to -198.2 °C and six Linde-Hampson cascade cycles for more cooling to -252.2 °C. A novel 130 TPD hydrogen liquefaction concept, including a single MR cycle, is proposed [20]. Cardella et al. [21] studied a novel approach for the development of large-scale plants. Yin et al. [22] proposed a hydrogen liquefaction plant based on liquid nitrogen pre-cooling and helium refrigeration. The coefficient of performance (COP) and specific energy consumption (SEC) were reported as 7.13 kWh/kg_{LH2} and 0.17, respectively.

Kramera et al. [23] studied a large-scale hydrogen supply chain for automotive applications and discovered that hydrogen distribution in the liquid state might be competitive to the compressed state. Kuendig et al. [24] studied the integration of liquid natural gas as pre-cooling into the hydrogen liquefaction plant and found it is enormously useful to decrease power input and construction cost. Yang et al. [25] developed a new conceptual design with a capacity of 300 TPD for hydrogen liquefaction integrated with a steam methane reforming process. It employs cold energy from the vaporization of liquefied natural gas (LNG) for the pre-cooling of hydrogen. Mehrpooya et al. [26] developed an integrated process with 290 and 296 TPD of production capacity for liquid hydrogen and natural gas, respectively. They employed two different MR with novel compositions and achieved 0.2442 for COP. Chang et al. [27] investigated the concept of using cold energy of LNG for pre-cooling of hydrogen, aiming at minimizing power consumption in hydrogen liquefiers. They found that LNG at atmospheric pressure is much more effective in pre-cooling than pressurized LNG and identified a 2-stage expansion cycle as the most suitable one for the pilot system.

Beylakov et al. [28] proposed a low-capacity concept with helium cooling, six helium-hydrogen heat exchangers (HXs), and six ortho-para converters. The problems of liquid parahydrogen production by catalytic ortho-para conversion at cryogenic temperatures were studied [29]. Skaugen et al. [30] investigated using catalyst-filled plate-fin and spiral-wound heat exchangers for hydrogen liquefaction applications. An advanced hydrogen liquefaction system with catalyst-infused HXs was investigated energetically and exegetically [31]. Different pre-cooling alternatives, including typical conversion of hydrogen to parahydrogen, were considered and found that energy and exergy efficiencies are 15.4% and 11.5%, respectively. Ansarinasab et al. [32] showed that HXs are responsible for the highest exergy destruction in hydrogen liquefaction plants. Different analysis methods,

[1] World Energy NETwork

such as exergy, exergoeconomic, and exergy-environmental for hydrogen liquefaction plants, were investigated [33].

Kuz'menko [34] designed a medium-capacity hydrogen liquefier with a mixture of helium and nitrogen as the refrigeration system. The average SEC and thermodynamic efficiency of the plant have been reported as 13.85 kWh/kg_{LH_2} and 34.6% in turn. A small-scale hydrogen liquefaction plant with 3 TPD capacity and helium Brayton refrigeration was investigated [35]. The results showed that the initial cost and efficiency of the proposed liquefaction process are lower than that of large-scale plants. Kumar et al. [36] studied a helium refrigeration system with a capacity of 470 W at around 20 K for the field of hydrogen liquefaction application. Chang et al. [37] studied a thermodynamic analysis to design hydrogen liquefaction systems with helium or neon Brayton refrigerators for domestic applications in Korea. They showed that helium Brayton refrigerator operating at much lower pressures might be a good choice.

Stang et al. [38] developed a hydrogen liquefaction prototype unit at NTNU-SINTEF. They used a helium-neon mixture to pre-cool hydrogen from 25 °C to near −193 °C. The results showed that MR with high-temperature glide and a low freezing point could play a significant role in hydrogen liquefaction processes. Shimko and Gardiner [39] did the designation and construction of a small-scale pilot plant with a 20 kg/hr capacity as a model for scaling to a 50 TPD plant. They applied helium as a refrigerant to cool hydrogen from −193 °C to -253 °C. Krasae-in et al. [40] investigated a small-scale laboratory liquefier with a MR refrigeration system that could cool down 2 kg/hr of feed hydrogen gas to liquid hydrogen. A small-scale hydrogen liquefaction plant with a novel MR refrigeration cycle was constructed [41]. The experiments showed that hydrogen MR pre-cooling is preferred for liquefaction since it performs more efficiently than conventional ones [41]. Asadnia et al. [42] carried out a historical review of hydrogen liquefaction systems and different hydrogen production methodologies. They introduced a novel classification of hydrogen liquefaction and reviewed hybrid conceptual plants.

Environmental problems and high energy costs have directed attention to using renewable energy sources such as geothermal and solar for different applications. Ratlamwala et al. [43] studied thermodynamic investigation of a novel integrated process for three main outputs, including liquid hydrogen, electricity, and cooling. They analyzed the impact of different design indicators such as geothermal water temperature, reference temperature, and working fluid concentration on the system. Yilmaz et al. [44] analyzed the economic aspects of hydrogen production and liquefaction. They employed a high-temperature steam electrolysis process for hydrogen production. Aasadnia and Mehrpooya [45] proposed an innovative conceptual design for hydrogen liquefaction with the help of an absorption refrigeration system (ARS). They used solar energy for feeding the ARS and reported COP and SEC as 0.2034 and 6.47 kWh/kg_{LH_2}, respectively. A new configuration for hydrogen liquefaction integrated with solar ARS and organic Rankin cycle was proposed [46]. The COP and SEC were reported as 0.202 and 4.02 kWh/kg_{LH_2}, respectively. Asadnia et al. [47] investigated a hydrogen liquefaction cycle with two ammonia ARSs from exergy, exergoeconomic, and exergoenvironmental aspects. The ARSs were fed by geothermal energy, and the capacity was 260 TPD. Kaska et al. [48] utilized a geothermal energy source with a temperature of 200 °C for hydrogen liquefaction. High-temperature geothermal water was used for pre-cooling of hydrogen down to -30 ° [49]. A novel geothermal-based multigeneration system was suggested for producing multiple commodities [50]. Yilmaz [51] modeled a hydrogen liquefaction process assisted by geothermal energy. He used geothermal energy for precooling and producing work through a binary geothermal cycle. For minimizing the unit cost, exergoeconomic optimization was applied using a genetic algorithm method. Seyam et al. [52] presented a 335 TPD hydrogen liquefaction system combined with a geothermal and isobutene power plant. In this concept hydrogen Claude refrigeration system and nitrogen precooling were utilized. The total power consumption and SEC of the process were reported as 107 MW and 6.41 kWh/kg-LH_2, respectively. Nouri et al. [53] proposed a hybrid structure for simultaneous production of liquid hydrogen and carbon dioxide. Hydrogen and oxygen were produced by a photovoltaic electrolyzer. The payback of the plant was estimated as 4.79 years. Bae et al. [54] used genetic algorithm for multi-objective optimization for hydrogen liquefaction process integrated with LNG system. The results showed that the 38% reduction in CO_2 emissions could lead to 45% and 4% rise in the total investment cost and SEC respectively. Ghorbani et al. [55] proposed an integrated system composed of four subsystems to use the waste heat in other integrated structures at the time of liquefying hydrogen. They used Aspen HYSYS for hydrogen liquefaction section and applied Peng-Robinson (P-R) equation of state (EOS) for simulation of the whole process.

This study is dedicated to modifying a new conceptual design by investigating and modifying the liquefaction process proposed by Sadaghiani et al. [56]. The novelty of this work lays in the

new configuration and new MR compositions. Moreover for increasing the accuracy of the results two different EOSs has been applied instead of using one EOS for the whole process, Modified-Benedict–Webb–Rubin (MBWR) EOS is applied to the hydrogen streams, while for the other streams in the process, P-R is used as suggested by Rezaie Azizabadi et al. [57] and Berstad et al. [58]. Using these two EOSs could improve the overall results and lead to more accurate data for conversion of ortho-para [57-58]. The air cooler's consumption power is integrated, while for the base concept, it was ignored. The critical operating parameters such as temperature levels, lower and higher pressure levels, and the number of compressors are determined so that they lead to a lower SEC. These items are integrated intensively; so, the process is done through trial and error; a simple and effective method. The exergy and energy analysis is applied to the process while simplification assumption in the base concept are improve to increase the results. The chemical and physical exergy are considered and none of the components is ignored. The final process is compared to the base one, and exergy and energy analysis are discussed. The base concept has been utilized in many researches so it will be of great importance to improve this concept since could affect many of the reseaches that will use this concept.

2. Methodology and process description

The base concept shown in Figure 1 comprises two independent sections; pre-cooling and liquefaction. The choice of intermediate temperature between pre-cooling and liquefaction is of great importance. Lower temperature transfers more loads to the liquefaction section, which experiences lower efficiency. Higher temperature will limit the selection of MR components while choosing improper components due to the low solidification temperature leads to crucial problems in the process. Stang et al. [38], Shimko and Gardiner [39], and Krasae-In et al. [14] took −193 °C for this purpose, while a temperature near -198 °C is appointed by Asadnia et al. [19] and Berstad et al. [13]. In large hydrogen liquefaction plants, such as Ingolstadt, a nitrogen refrigeration system is utilized for pre-cooling hydrogen gas from 25 °C to equilibrium hydrogen gas at -198 °C [59]. Here pre-cooling section cools feed hydrogen with a pressure equal to 21 bar from 25 °C to -195 °C, and the liquefaction section is dedicated to cooling from -195°C to -253°C. Pressure higher than 15 bar as supercritical pressure avoids condensation [56], at the same time higher feed pressure leads to lower power input [9, 10, 12]. The MR utilized in the pre-cooling section comprises nine components, listed in Table 1, and is compressed from 2 bar to 16 bar through two steps. The first step is done through a compressor (Com 1); however, the second step includes a pump and a compressor (Com 2).

Table 1- Composition of the MR utilized in the pre-cooling section [56].

Components	Mole fraction (%)	Components	Mole fraction (%)
Methane	17.00	Propane	18.00
Ethane	7.00	n-Pentane	15.00
n-Butane	2.00	R-14	8.00
Hydrogen	1.00	Ethylene	16.00
Nitrogen	16.00		

Outputs of these devices (pump and com 2) are mixed and entered into Separator-2 as the stream (M1). Then, outflows of the separator 2 move into HX-1 as M2 (gas) and M3 (liquid) to cool down the hydrogen stream to -45 °C. Two more HXs and three turbo-expanders (Exp-1, Exp-2, and Exp-3) are employed to yield stream H4 at -195 °C.

The MR used in the liquefaction section comprises 6.5% hydrogen, 10% neon, and 83.5% helium. The MR stream (N5) is compressed from 1 bar to 10 bar by passing through three compressors (Com-3, Com-4, and Com-5) and three coolers (Cooler 3, Cooler 4, and Cooler 5); later, the stream (N1) is divided into three new streams. Every stream goes through HX to be cooled with the return stream. Then they are introduced to turbo-expanders and HXs (HX4, HX5, and HX6) for cooling hydrogen to -253 °C. At -195 °C and -240 °C, two ortho-para converters are integrated into the cycle to yield liquid hydrogen with a 95% parahydrogen concentration. The cooled hydrogen stream (H9) is finally introduced to a turbo-expander (Exp7) to be expanded to 1.3 bar. The discharge stream of the expander (Exp7) is separated into liquid and vapor. The vapor fraction (H11) is sent to the ejector, and the liquid stream (H12) is delivered to the storage tank.

2.1. Ortho-para Conversion

Due to the relative orientation of the proton's spin in the nucleus, molecular hydrogen has two spin isomers named parahydrogen and orthohydrogen [60]. Orthohydrogen is composed of two atoms with similar spins, while parahydrogen includes two atoms with opposite spins. The equilibrium of ortho-para is a function of temperature [61], and orthohydrogen has a higher energy level. In-room conditions, the equilibrium consists of 75% orthohydrogen and 25% parahydrogen, known as normal hydrogen. Orthohydrogen converts to parahydrogen as the temperature decreases. The conversion of ortho-para has two significant effects, which should be considered in the liquefaction process [62].

1. It is s an exothermic reaction.
2. It occurs very slowly and needs to be accelerated by catalysts.

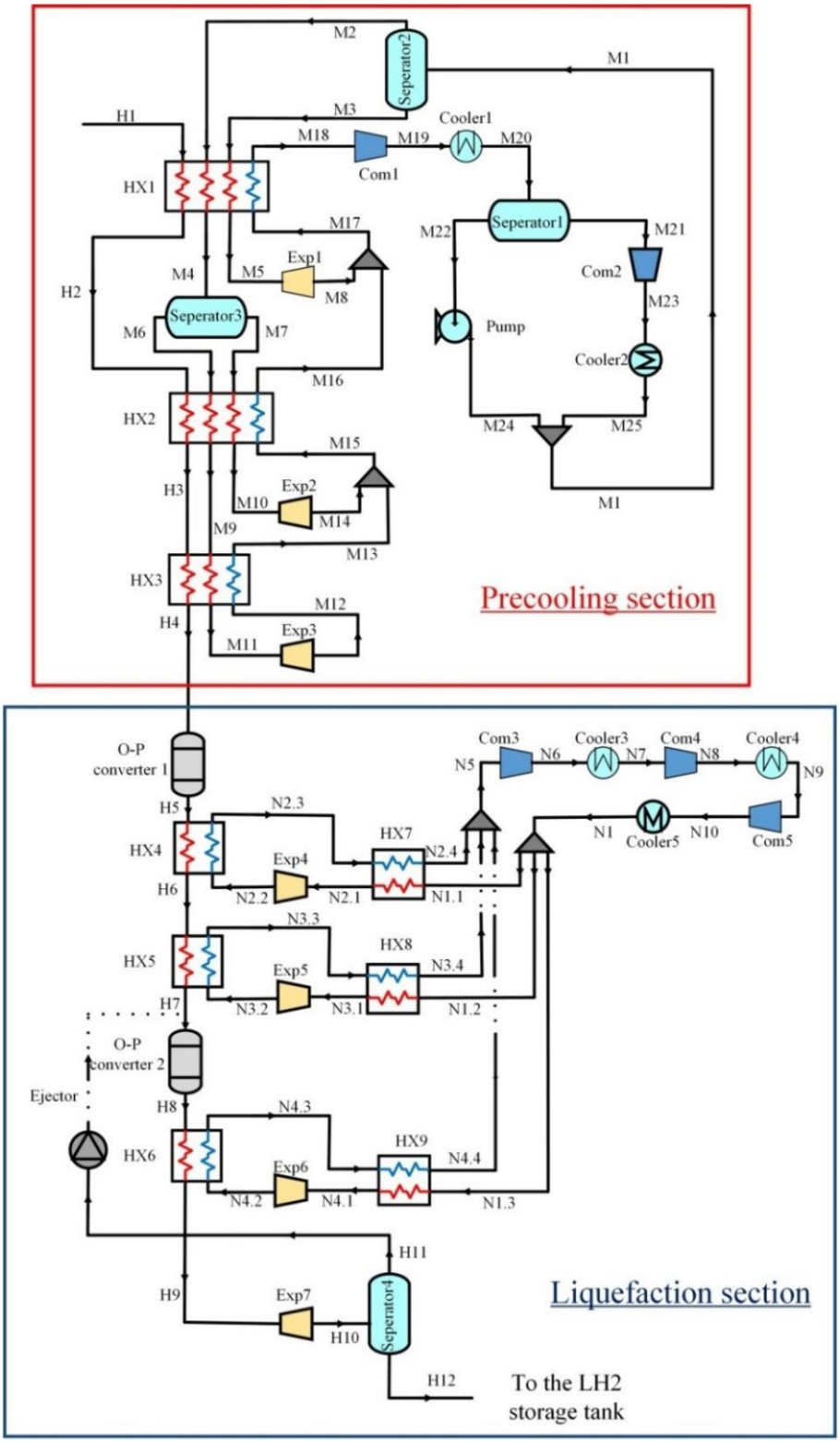

Figure 1- Flow-sheet of the base hydrogen liquefaction process [56].

If a catalytic conversion of ortho-para is not included, the natural conversion will not proceed at the proper rate; therefore, exothermic conversion of ortho-para releases heat and results in boil-off which leads to the evaporation of 50% and 65% of liquid hydrogen after 100 and 1000 hours, respectively [63]. Here two catalytic ortho-para converters at 78 k and 33 k are considered in the liquefaction section.

2.2. Process simulation and assumptions

In this study, the base concept is investigated using Aspen HYSYS V9. Its ability to simulate liquefaction processes has been utilized in many researches [26, 46, 64, 65]. In the first step, the base concept is simulated and investigated, then the configuration, working parameters, and the MR composition are determined to reach a new concept with higher efficiency.

Most of the assumptions considered in this study are the same as the base concept [56] and are presented below:

- The reference condition is 25 °C and 101.3 kPa, and pressure losses are ignored.
- The components are working in steady-state and steady flow conditions.
- HXs, compressors, and turbo-expanders are assumed adiabatic.
- Pinch temperatures are adjusted between 1 °C and 3 °C as recommended by Barron for cryogenic processes [66].
- Kinetic and potential terms in the energy and exergy balance equations are negligible.
- Compressor, pump, and turbo-expander efficiencies are set as 90%, 90%, and 85%, respectively

It deserves to note that the efficiency of the compressors, pumps, and expanders could affect the overall efficiency of the concept crucially, so they should be similar to the base concept to be able to have a fair comparison. In the base concept, the P-R equation of state is applied for the whole process, while it could not estimate important parameters for applications like hydrogen liquefaction that experiences extremely low temperatures. Rezaie Azizabadi et al. [65] show that MBWR could be a perfect choice for hydrogen in the temperature ranges typically met in the liquefaction, while P-R could not yield reliable data for this range of temperature. Although P-R could not perform well for estimating data in hydrogen streams, it has been used for the whole process in many studies conducted on hydrogen liquefaction [26, 45-47, 56, 64] due to its simplicity. Rezaie Azizabadi et al. [65] have investigated four different EOSs and found that MBWR for hydrogen liquefaction applications could yield the most accurate results. In Figure 2, the results of Aspen HYSYS for conversion enthalpy using MBWR are compared to the experimental data. Here P-R is used for MR streams, while the MBWR is applied to hydrogen streams to obtain more accurate results.

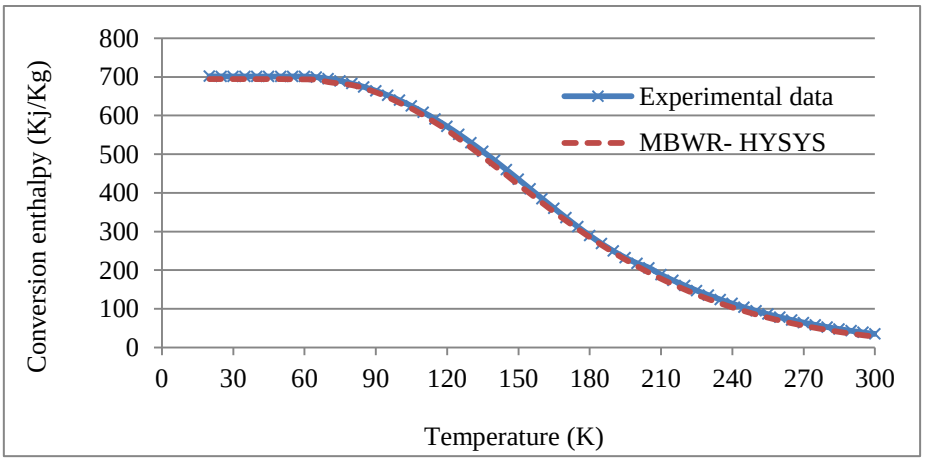

Figure 2. Comparison of experimental data for conversion enthalpy [65] to Aspen HYSYS results using MBWR as a fluid package.

3. Energy and Exergy analysis

Using the first law of thermodynamics in estimating power consumption and efficiency of the process is called energy analysis. It balances the useful output energy with the input energy and involves mass and energy balances as of the governing equations. Mass and energy balances lead to the following equations for a general control volume in the steady-state condition and ignorable kinetic and potential energy.

$$\sum \dot{m}_{in} = \sum \dot{m}_{out} \quad (1)$$

$$\dot{Q} - \dot{W} = \sum \dot{m}_{out} h_{out} - \sum \dot{m}_{in} h_{in} \quad (2)$$

There are two important quantitative indexes in energy analysis, SEC and COP [67], which are defined as below:

$$COP = \frac{Total\ rate\ of\ rejected\ heat\ from\ hydrogen}{Total\ rate\ of\ consumped\ energy\ in\ components} = \frac{\dot{m}_F\,(h_F - h_P)}{\dot{W}_{net}} \quad (3)$$

$$SEC = \frac{Net\ power\ consumption}{Mass\ flow\ rate} = \frac{\dot{W}_{net}}{\dot{m}_F} \quad (4)$$

Where

$\dot{m}_F$: Mass flow rate of feed hydrogen.

h_F/h_P: Mass enthalpy of feed/product hydrogen.

$\dot{W}_{net}$: Net power consumption rate of the process.

Energy analysis is widely used to evaluate thermodynamic systems. It could not show how

or where irreversibility occurs in a system, so the exergy analysis should be employed [68]. Exergy is the amount of available energy or measure of the energy quality within a system. This analysis indicates in which direction efforts should be concentrated to improve the system's performance [69]. In the absence of nuclear, magnetic, electrical, and surface-tension effects, the total exergy of a system E_{sys} consists of physical exergy E_{ph}, chemical exergy E_{ch}, kinetic exergy E_{ki}, and potential exergy E_{po} [70]. For the liquefaction processes, the changes in kinetic and potential exergy could be neglected compared to the chemical and physical exergy, so the total exergy of the system is as follows. It must be noted that when considering the conversion of energy inside components such as turbo-compressors, cryo-expanders, and ejectors, this is not a valid assumption [58].

$$E_{sys} = E_{ph} + E_{ch} = \dot{m}\,(e_{ph} + e_{ch}) \tag{5}$$

The rate of physical exergy associated with the material stream is:

$$E_{ph} = \dot{m}[(h - h_0) - T_0(s - s_0)] \tag{6}$$

The subscript 0 refers to the property values at the dead point, $T_0 = 298.15\,K$ and $P_0 = 1.013\,bar$. The chemical exergy rate for a mixture of N ideal gases is as follows [70]:

$$E_{ch} = \dot{m}(e_{ch}) = \dot{m}\left[\sum_{i=1}^{N} x_i \bar{e}_i^0 + \bar{R}T_0 \sum_{i=1}^{N} x_i \ln(x_i)\right] \tag{7}$$

Where $\bar{e}_i^0$ and x_i are the standard molar chemical exergy and mole fraction of the ith component, respectively. $\bar{R}$ is the molar ideal-gas constant and is 8.3144 kJ/kmolK. For all substances dealt with in this study, standard chemical exergy could be gained from the literature except R14 and parahydrogen. For these two materials, the chemical exergy could be calculated by defining a reaction and using the Gibbs free energy of formation described by Kotas [71].

Considering a control volume at steady-state, exergy balance can be expressed as:

$$\dot{m}e_{in} + \dot{E}x_{Q\,in} = \dot{m}e_{out} + \dot{E}x_{Q\,out} + \dot{W} + \dot{I} \tag{8}$$

Exergy losses due to irreversibility in the steady state for each component are defined as follows [71].

$$\dot{I} = T_0\left[\sum_{out} \dot{m}s - \sum_{in} \dot{m}s - \sum_{hs} \frac{\dot{Q}}{T_{hs}}\right] \tag{9}$$

Definitions of exergy destruction and exergy efficiency for different components are presented in Table 2.

Table 2 - Exergy relations for different components in the liquefaction process.

Equipment	Exergy destruction & exergy efficiency
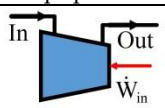 Compressor	$\dot{I}_{Com} = (\dot{m}e)_{In} + \dot{W}_{In} - (\dot{m}e)_{Out}$ $\varepsilon_{Com} = \frac{(\dot{m}e)_{Out} - (\dot{m}e)_{In}}{\dot{W}_{In}}$
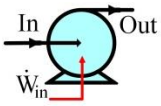 Pump	$\dot{I}_{Pump} = (\dot{m}e)_{In} + \dot{W}_{In} - (\dot{m}e)_{Out}$ $\varepsilon_{Pump} = \frac{(\dot{m}e)_{Out} - (\dot{m}e)_{In}}{\dot{W}_{In}}$
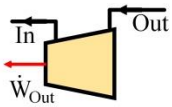 Expander	$\dot{I}_{Exp} = (\dot{m}e)_{In} - \dot{W}_{Out} - (\dot{m}e)_{Out}$ $\varepsilon_{Exp} = \frac{\dot{W}_{Out}}{(\dot{m}e)_{In} - (\dot{m}e)_{Out}}$
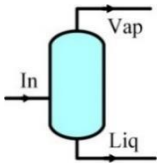 Separator	$\dot{I}_{Sep} = (\dot{m}e)_{In} - (\dot{m}e)_{Vap} - (\dot{m}e)_{Liq}$ $\varepsilon_{Sep} = \frac{(\dot{m}e)_{Vap} + (\dot{m}e)_{Liq}}{(\dot{m}e)_{In}}$

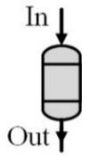 Ortho-para converter	$\dot{I}_{Con} = (\dot{m}e)_{In} - (\dot{m}e)_{Out}$ $\varepsilon_{con} = \frac{(\dot{m}e)_{Out}}{(\dot{m}e)_{In}}$
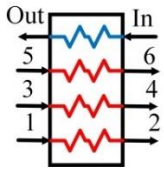 Heat Exchanger (Cold Stream: In/Out) (Hot Stream: 1/2, 3/4, 5/6)	$\dot{I}_{HX} = \sum(\dot{m}e)_{In} - \sum(\dot{m}e)_{Out} = (\dot{m}e)_1 + (\dot{m}e)_3 + (\dot{m}e)_5 + (\dot{m}e)_{In} - (\dot{m}e)_2 - (\dot{m}e)_4 - (\dot{m}e)_6 - (\dot{m}e)_{Out}$ $\varepsilon_{HX} = \frac{(\sum(\dot{m}e)_{In} - \sum(\dot{m}e)_{Out})_{Hot\ Streams}}{(\sum(\dot{m}e)_{In} - \sum(\dot{m}e)_{Out})_{Cold\ Streams}} = \frac{(\dot{m}e)_1 + (\dot{m}e)_3 + (\dot{m}e)_5 - (\dot{m}e)_2 - (\dot{m}e)_4 - (\dot{m}e)_6}{(\dot{m}e)_{In} - (\dot{m}e)_{Out}}$
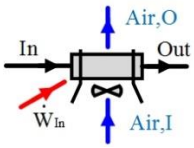 Air cooler [47]	$\dot{I}_{Air\ cooler} = (\dot{m}e)_{In} + (\dot{m}e)_{Air,I} + \dot{W}_{In} - (\dot{m}e)_{Out} - (\dot{m}e)_{Air,O}$ $\varepsilon_{Air\ cooler} = \frac{(\dot{m}e)_{Out} - (\dot{m}e)_{Air,O}}{(\dot{m}e)_{In} - (\dot{m}e)_{Air,I} + \dot{W}_{In}}$
Process [56]	$\dot{I}_{process} = Summation\ of\ irreversibility\ of\ all\ devices$ $\varepsilon_{process} = \frac{Total\ exergy\ output}{Total\ exergy\ input} = 1 - \frac{Total\ irreversibillity\ of\ process}{Total\ exergy\ input\ to\ process}$

4. Modifying the base concept

In the first step, the base concept with the same parameters and assumptions is simulated in Aspen HYSYS V9. to investigate the assumptions and reported data. The simulation results in the pre-cooling section are the same as the base concept; however, there is a considerable inconsistency between the liquefaction section results. A meticulous investigation shows that the primary reason for this inconsistency lies in the simulation of ortho-para conversion. Inlet and outlet temperatures of the ortho-para converters for the base concept and two simulated cases with P-R and MBWR as a fluid package are presented in Table 3. The parahydrogen fraction in the outlet stream of the Ortho-para Converter 1 and Ortho-para Converter 2 is 50% and 95% in turn.

Table 3 - Inlet and outlet temperatures of the ortho-para converters in the base concept and two simulated cases in Aspen HYSYS with P-R and MBWR as a fluid package.

		Base Concept [56]	P-R	MBWR
Ortho-para Converter 1	Inlet temperature °C	-195	-195	-195
	Outlet temperature °C	-195	-189.5	-181.3
Ortho-para Converter 2	Inlet temperature °C	-240	-240	-240
	Outlet temperature °C	-240	-235.2	-231.2

The outlet temperature for ortho-para converters in the base concept is different from the two simulated cases. It seems that in the base concept the converters are considered as a constant temperature that is not compatible with physical concepts. Due to the exothermic reaction in the ortho-para converter and adiabatic assumption, it should be accompanied by a temperature rise. Here MBWR is employed to estimate conversion enthalpy since it is proved in the previous research that it leads to a more accurate simulation for hydrogen liquefaction processes [65].

The base concept with confirmed assumptions for the pre-cooling and liquefaction sections is used to modify a new concept with lower SEC and higher COP through exploring the below items:

1. The number of compressors.
2. Configuration modification.
3. Higher and Lower pressure levels.
4. Temperature levels.
5. MR composition.

As some of the considered parameters are interlinked and depend on each other, determining their optimum values should be done in a repetitive manner and step by step.

4.1. Number of compressors

The number of compressors could be determined independent of the other parameters, so in the first step, it is investigated. The total power consumption for the compression stages, average

output temperature, and compression ratio are selected as the comparison indexes for choosing the number of compressors. In the pre-cooling section, 4 cases with 1 to 4 compression stages, and in the liquefaction section, 6 cases with 1 to 6 compressors are investigated. The cases with more than one compression stage should be optimized for the intermediate pressure. The optimum pressure for two simple compression stages with an intercooler is as follows:

$$P_2^2 = P_1 . P_3 \quad (10)$$

With some manipulating for the case in which there are n compressors and n intercoolers, the optimum pressure in the stage i[th] could be defined as follows:

$$P_i^{n-i+1} = P_{i-1}^{n-1} . P_n \quad (11)$$

As the compressors are not simply series in the pre-cooling section, a trial and error procedure, which is functional and straightforward [45], has been utilized for finding the optimum number of compressors. The results are presented in Figures 3 to 6.

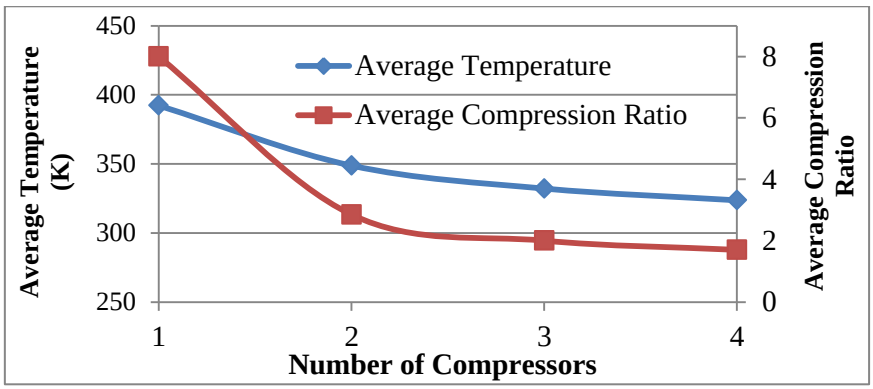

Figure 3 - Average temperature and average compression ratio for different numbers of compressors in the pre-cooling section.

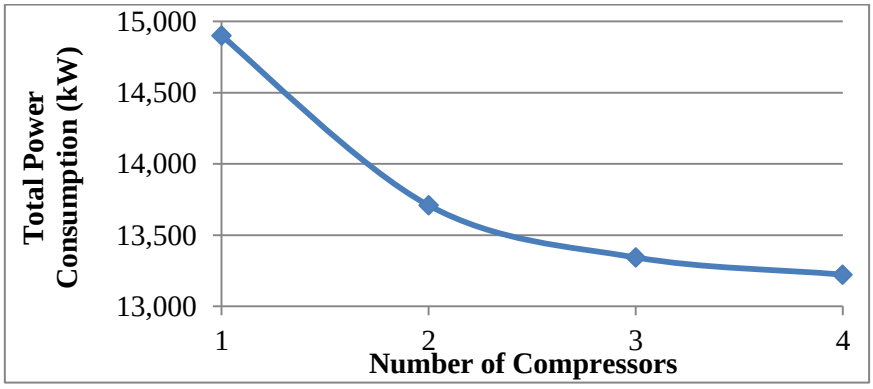

Figure 4 - Total power consumption for different numbers of compressors in the pre-cooling section.

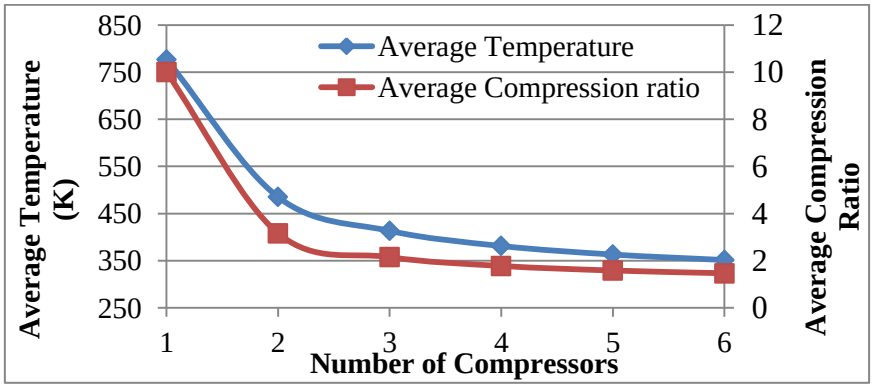

Figure 5 - Average temperature and average compression ratio for different numbers of compressors in the liquefaction section.

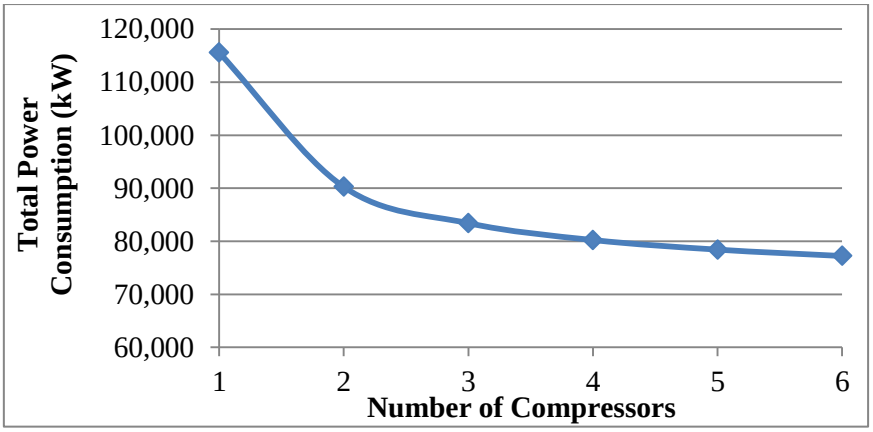

Figure 6 - Total power consumption for different numbers of compressors in the liquefaction section.

Increasing the number of compressors could reduce the total power consumption, average outlet temperature, and compression ratio of compressors while increasing the initial cost. Therefore, finding the best number of compressors is of great importance. Based on the curves shown in Figure 4 and Figure 5, it is found that just increasing the number of compressors to three could affect the power consumption significantly, while increasing more could not create a sensible improvement. Therefore, the optimum number of compressors in the pre-cooling section is 3. Similarly, concerning Figure 6 and Figure 7, the optimum number of compression stages for the liquefaction section is 4. The number of compressors is independent of other parameters, so the presented numbers for compressors in pre-cooling and liquefaction sections are final.

4.2. Configuration modification

Different configurations for the pre-cooling and liquefaction sections are investigated by relocating the compressors, pumps, coolers, and separators. Results are compared to the base concept to find the best possible configuration. It could be found that any change to the configuration could lead to a significant difference in the process efficiency. In the base concept, the power consumption of the coolers is ignored, while in this study, as depicted in Figure 7, coolers are replaced with air coolers, and their power consumption are considered. This could lead to more accurate results.

4.3. Pressure and temperature levels and MR composition

Pressure levels, temperature levels, and MR composition are important since they affect the plant's SEC and COP. Due to several linked equipment in the process, the considered parameters depend on each other; therefore, any change to one could affect the optimum value of the others. Besides, for a successful run in the simulator and to achieve reliable data, all the limitations should be met simultaneously. A trial and error method is used in this study, since using a model-based optimization would be complicated and may improve the results just slightly [45]. The trial and error method is a simple and functional method and has been utilized in many similar studies [14, 45, 46]. Therefore, the considered parameters, including pressure levels, temperature levels, and MR composition, are changed in a repetitive procedure with small increments aiming at minimizing SEC. Every change is followed by a simulator run to check the SEC and see that the minimum approach temperature for all heat exchangers remains in the acceptable range.

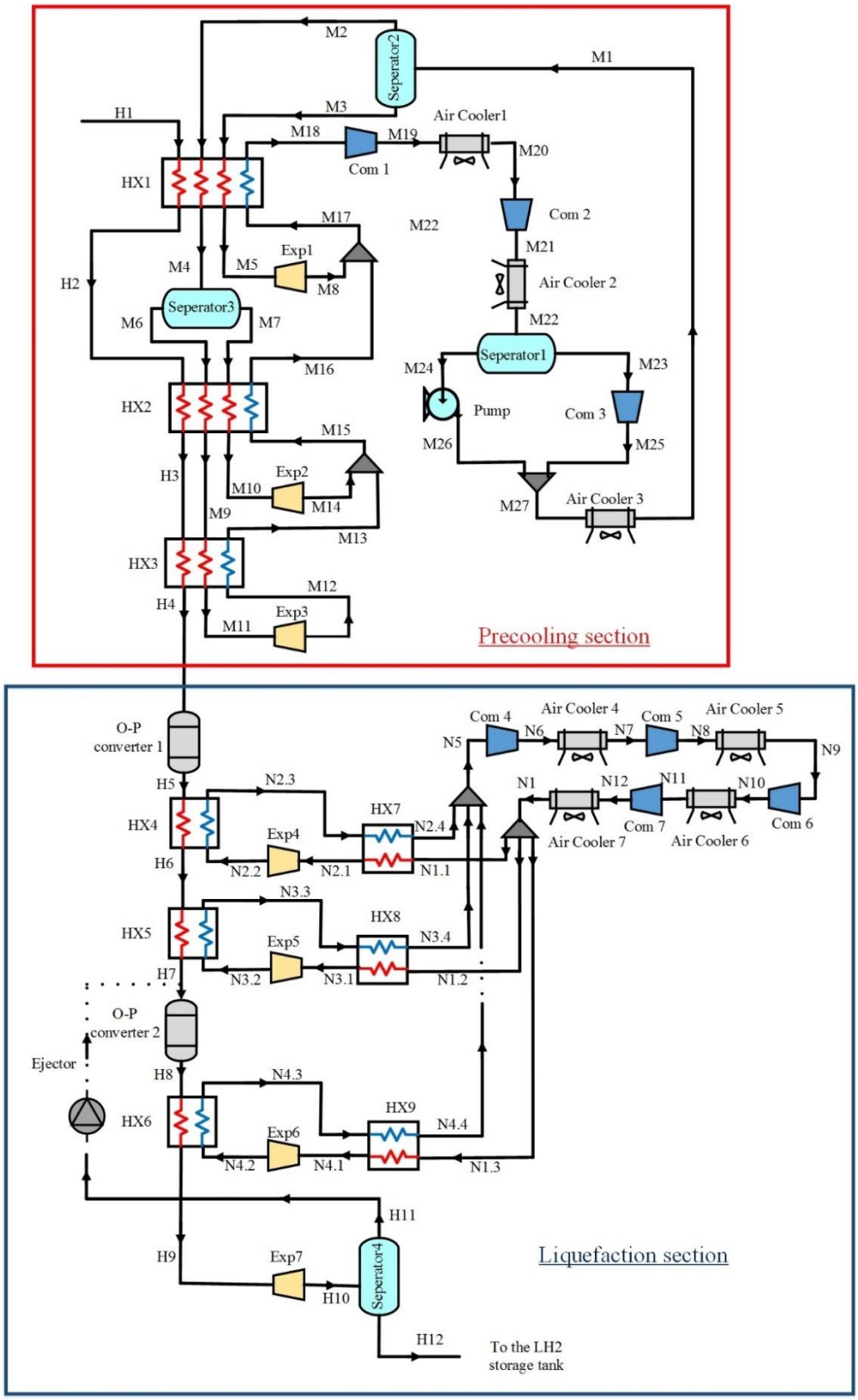

Figure 7 – Flow-sheet of the new concept.

The effects of lower and upper-pressure levels on the SEC are investigated in 3 different manners. In the two first cases, the higher and lower levels are changed separately; however, the third manner includes a constant pressure difference. Lower and higher levels of the pre-cooling section are altered in the range of 1 to 3 bar and 15 to 17 bar, respectively. For the

liquefaction section, these ranges are 0.2 to 2 bar and 9 to 11 bar. Investigations show that lower pressure levels are more impactful than higher pressure levels in both pre-cooling and liquefaction sections. The temperature levels of HXs are changed in the same way to yield minimum SEC. In the next step, MR composition in the pre-cooling and liquefaction sections should be determined. Although determining MR composition through a trial and error procedure is time-consuming and boring, it could yield desirable results.

5. Results and discussion

The final MR composition in the pre-cooling and liquefaction sections is presented in Table 4. The thermodynamic properties of the newly developed concept, including pressure, temperature, mass flow rate, and physical and chemical exergies for the pre-cooling and liquefaction sections, are presented in Tables 5 and 6 in turn.

The results show that chemical exergy in the liquefaction process is essential and should be considered since the intense changes through ortho-para converters and separators could affect the results crucially. Power consumption, exergy efficiency, and exergy destruction for different equipment of the process are presented in Table 7. The fraction of exergy destruction for component i is defined as follows and shown in Table 7 to have a better understating of the exergy destruction.

$$Y_{D,i} = \frac{\dot{I}_i}{\dot{I}_{Total}} \times 100 \quad (12)$$

Table 4. Final MR compositions in the pre-cooling and liquefaction sections.

Pre-cooling section	
Methane	0.165
Ethane	0.084
n-Butane	0.039
Hydrogen	0.007
Nitrogen	0.145
Propane	0.175
n-Pentane	0.155
Refrig-14	0.080
Ethylene	0.150
Liquefaction section	
Hydrogen	0.080
Helium	0.890
Neon	0.030

Table 5 - Thermodynamic properties for the pre-cooling streams in the new concept.

Stream No.	Temperature (°C)	Pressure (bar)	Mass flow ($kg.s^{-1}$)	Physical Exergy (kW)	Chemical Exergy (kW)	Total Exergy (kW)
			Pre-cooling section			
H1	25	21	3.45	12,964	404,023	416,987
H2	-51.6	21	3.45	13,492	404,023	417,515
H3	-104	21	3.45	14,803	404,023	418,826
H4	-195	21	3.45	20,669	404,023	424,692
M1	25	16	83.9	12,434	3,034,275	3,046,709
M2	25	16	28.76	1,219	1,675,941	1,677,160
M3	25	16	55.14	10,102	1,359,053	1,369,155
M4	-51.6	16	55.14	12,484	1,675,941	1,688,425
M5	-51.6	16	28.76	1,921	1,359,053	1,360,974
M6	-51.6	16	29.6	6,672	589,717	596,389
M7	-51.6	16	25.53	4,769	1,086,714	1,091,483
M8	-55.51	1.9	28.76	1,838	1,359,053	1,360,891
M9	-104	16	29.6	9,990	589,717	599,707
M10	-104	16	25.53	6,132	1,086,714	1,092,846
M11	-195	16	29.6	19,924	589,717	609,641
M12	-196.1	1.9	29.6	19,832	589,717	609,549
M13	-106.7	1.9	29.6	3,442	589,717	593,159
M14	-108.8	1.9	25.53	6,056	1,086,714	1,092,770
M15	-105.3	1.9	55.14	10,504	1,675,941	1,686,445
M16	-56.31	1.9	55.14	4,302	1,675,941	1,680,243
M17	-53.32	1.9	83.9	7,202	3,034,275	3,041,477
M18	15.01	1.9	83.9	3,119	3,034,275	3,037,394
M19	47.89	3.9	83.9	6,703	3,034,275	3,040,978
M20	25	3.9	83.9	6,593	3,034,275	3,040,868
M21	59.03	8	83.9	10,227	3,034,275	3,044,502
M22	25	8	83.9	9,791	3,034,275	3,044,066
M23	25	8	66.9	8,737	2,221,252	2,229,989
M24	25	8	17	290	337,925	338,215
M25	62.86	16	66.9	11,734	2,221,252	2,232,986
M26	25.41	16	17	312	337,925	338,237
M27	48.38	16	83.9	12,728	3,034,275	3,047,003

Table 6 - Thermodynamic properties for the liquefaction streams in the new concept.

Stream No.	Temperature (°C)	Pressure (bar)	Mass flow ($kg.s^{-1}$)	Physical Exergy (kW)	Chemical Exergy (kW)	Total Exergy (kW)
			Liquefaction section			
H5	-181.3	21	3.45	19,724	401,333	421,057
H6	-220	21	3.45	25,119	401,333	426,452
H7	-240	21	3.45	36,329	401,333	437,662
H8	-231.2	21	3.45	29,594	403,137	432,731
H9	-253	21	3.45	43,505	403,137	446,642
H10	-253.4	1.2	3.45	43,194	403,137	446,331
H11	-253.4	1.2	0	0	0	0
H12	-253.4	1.2	3.45	43,194	403,137	446,331
N1	25	10	41.5	54,407	431,778	486,185
N2.1	-181	10	7.5	15,195	78,032	93,227
N2.2	-227.5	1	7.5	11,333	78,032	89,365
N2.3	-182.5	1	7.5	5,411	78,032	83,443
N2.4	23.97	1	7.5	-56	78,032	77,976
N3.1	-221.3	10	14.5	38,903	150,862	151,251
N3.2	-247.7	1	14.5	32,944	150,862	183,806
N3.3	-223.3	1	14.5	20,329	150,862	171,191
N3.4	23.92	1	14.5	-109	150,862	150,753
N4.1	-234	10	19.5	59,358	202,883	262,241
N4.2	-254.2	1	19.5	52,280	202,883	255,163
N4.3	-236.5	1	19.5	34,866	202,883	237,749
N4.4	23.83	1	19.5	-147	202,883	202,736
N5	23.89	1	41.5	-312	431,778	431,466
N6	108.5	1.8	41.5	15,687	431,778	447,465
N7	25	1.8	41.5	13,654	431,778	445,432
N8	107.9	3.2	41.5	29,332	431,778	461,110
N9	25	3.2	41.5	27,328	431,778	459,106
N10	108.2	5.7	41.5	43,077	431,778	474,855
N11	25	5.7	41.5	41,052	431,778	472,830
N12	105.8	10	41.5	56,316	431,778	488,094

Table 7 - Exergy efficiency, exergy destruction, power consumption, and exergy destruction share for different process equipment.

Equipment	Power (kW)	ε (%)	$\dot{I}$ (kW)	Y_D (%)
Com1	3,953.4	90.7	369.4	0.98
Com2	3,997.5	90.9	363.5	0.97
Com3	3,286.6	91.2	289.6	0.77
Com4	17,369.6	92.1	1,370.6	3.64
Com5	17,024.9	92.1	1,346.9	3.58
Com6	17,092.2	92.1	1,343.2	3.57
Com7	16,596.4	92.0	1,332.4	3.54
Pump	25.3	87.1	3.3	0.01
Sum	79,345.8		6,418.8	17.05
Air Cooler 1	35.4	96.6	54.7	0.15
Air Cooler 2	83.3	90.5	32.1	0.09
Air Cooler 3	90.3	95.2	147.5	0.39
Air Cooler 4	55.5	74.8	141.2	0.38
Air Cooler 5	55.5	86.6	141.1	0.37
Air Cooler 6	55.6	90.8	140.7	0.37
Air Cooler 7	55.6	93.3	139.1	0.37
Sum	431.2		796.5	2.12
Exp1	-66.5	80.1	16.5	0.04
Exp2	-58.1	76.4	17.9	0.05
Exp3	-53.6	58.3	38.4	0.10
Exp4	-1,703.9	44.1	2,158.1	5.73
Exp5	-1,820.7	30.6	4,138.3	10.99
Exp6	-1,826.3	25.8	5,251.7	13.95
Exp7	-79.9	25.7	231.1	0.61
Sum	-5,608.9		11,852.1	31.48
HX1	0	89.7	421.3	1.12
HX2	0	96.7	204.9	0.54
HX3	0	96.4	595.8	1.58
HX4	0	91.2	523.6	1.39
HX5	0	88.7	1,420.1	3.77
HX6	0	79.9	3,502.5	9.30

HX7	0	98.0	107.0	0.28
HX8	0	97.3	552.2	1.47
HX9	0	96.5	1,226.0	3.26
Sum	0		8,553.4	22.72
Separator 1	0	~ 100.0	510.7	1.36
Separator 2	0	~ 100.0	394.0	1.05
Separator 3	0	~ 100.0	553.0	1.47
Sum	0		1,457.7	3.87
O-P converter 1	0	~ 100.0	3,635.0	9.66
O-P converter 2	0	~ 100.0	4,931.0	13.10
Sum	0		8,566.0	22.75
Total Sum	74,168.1		37,644.5	100.00

In the base concept, it is assumed that the power consumption of the air coolers is ignorable. The results show that it could be a valid assumption as the total power consumption of the air cooler is 431.2 kW, less than 0.6% of the total power consumption of the process. Meanwhile, the exergy efficiency for air coolers is in the range of 74.8 to 96.6. They are responsible for up to 2.12% of the total exergy destruction in the process. Therefore, it may be better to consider the air cooler in exergy destruction. Sadaghiani et al. [56] had not evaluated separators and ortho-para converters by exergy analysis in their study. The exergy efficiency for these components is nearly 100%; however, the total exergy destruction for ortho-para converters and separators is responsible for 22.75% and 3.87% of the total exergy destruction, respectively. Expanders are the only components that, compared to the ortho-para converters, impose more exergy destruction on the process. Expanders have the lowest exergy efficiencies and highest exergy destruction. The heat exchangers are the third major source of exergy destruction in the considered process, followed by compressors (and pump), separators, and air coolers. The results show that chemical exergy for separators and ortho-para converters in the liquefaction process is of great importance. The main changes in chemical exergy for the liquefaction process occur in these components and could affect the total exergy destruction and exergy efficiency.

The SEC, COP, and exergy efficiency (ε) for the base concept and the modified new one are reported in Table 8. Results show that the new concept is improved compared to the base one so that the SEC is increased by 18.8%, and COP and exergy efficiency is decreased by 14.4% and 15.5% in turn.

Table 8 – Comparing the SEC, COP, and exergy efficiency of the new concept to the base one.

	Indexes	Base concept	New concept	New VS. Base (%)
Pre-cooling section	SEC (kWh/kg)	1.09	0.909	-16.6
	COP	0.803	0.893	11.2
	ε (%)	66.45	64.47	-3.0
Liquefaction section	SEC (kWh/kg)	6.26	5.06	-19.2
	COP	0.0713	0.083	16.4
	ε (%)	38.49	45.51	18.2
Complete liquefaction process	SEC (kWh/kg)	7.35	5.97	-18.8
	COP	0.180	0.206	14.4
	ε (%)	42.63	49.24	15.5

A comparison between the final concept of this study and the concept presented by Asadnia et al. [19] and Krasae-In et al. [14] is shown in Table 9. The COP of the new concept is the best, but for SEC and ε the concept proposed by Krasae-In et al. [14] seems to be better. It should be considered that the SEC of the present study compared to the existing plant such as Ingolstadt (13.58 kWh/kg) is much better.

Table 9 – Comparing the SEC, COP, and exergy efficiency of the new concept to other studies.

	Asadnia et al. [19]	Krasae-In et al. [14]	This study
SEC	7.69	5.35	5.97
COP	0.171	0.166	0.206
ε	39.5	56.9	49.24

6. Conclusion

A new 300 TPD conceptual plant for hydrogen liquefaction has been developed through parameter optimization and configuration modification of the base concept proposed by Sadaghiani et al. [56]. Aspen HYSYS V9. is utilized for simulation since it has been used for the base concept and many similar studies in the field of hydrogen liquefaction. Ortho-para conversion is simulated more accurately thanks to the using MBWR equation of state for hydrogen streams besides using P-R for other streams of the process and applying an adiabatic condition to the O-P Converters. Configuration of the process is improved by changing the location of different components in the process, such as compressors and coolers. The number of compression stages and intermediate pressure for every stage is improved. Operating parameters

and MR compositions for the new configuration are determined using a trial and error method, leading to a lower SEC for the whole process. This study is more accurate as two different EOS are employed, the power consumption for the coolers is considered, and exergy analysis is performed on all components even the ones that are ignored in similar studies.

The exergy efficiency for the air coolers is in the range of 74.8 to 96.6, and they are responsible for 2.12% of the total exergy destruction in the process. Moreover, the exergy analysis is applied to the ortho-para converters and separators. The results show that ortho-para converters and separators are responsible for 22.75% and 3.87% of the total exergy destruction, respectively, while their exergy efficiency is nearly 100%. Therefore, they should not be ignored in the exergy analysis as they could affect the exergy efficiency of the process. Configuration and essential parameters such as pressure levels and temperature levels are of great importance in the liquefaction process as small changes to them could lead to considerable changes in SEC and COP, so they are improved using the trial and error method. It should be noted that in both pre-cooling and liquefaction sections, lower pressure levels could affect the process efficiency more than higher pressure levels. The results show that the new concept enjoys higher efficiency and lower energy consumption. The SEC, COP, and ε of the final concept are 5.97 $kWhr/kg$, 0.206, and 49.24%, respectively, which shows 18.8%, 14.4%, and 15.5% improvement compared to the base concept. Although the process is improved in different aspects, the liquefaction section is still responsible for 85% of the total SEC, and it deserves to focus on this section for future studies. Utilizing systematic optimization methods and applying exergoeconomic and exergoenvironmental analysis to this concept are subjects that should be considered for future studies in this field as could yield useful data and results.

Nomenclature

Symbols					
e_x	specific exergy, kJ/kg	$\dot{E}x_Q$	exergy associated with the heat transfer	min	Minute
$\dot{m}$	mass flow rate, kg/s	hr	time, hour	P-R	Peng-Robinson
$\dot{E}_x$	the rate of exergy flow	ε	exergy efficiency	MBWR	Modified-Benedict–Webb–Rubin
e_{ph}	physical exergy, kW/kg	Abbreviations		Subscripts	
e_{ch}	chemical exergy, kW/kg	Com	compressor	In	inlet
h	specific enthalpy, kJ/kg	Exp	expander	Out	outlet
$\dot{I}$	exergy destruction, kW	HX	heat exchanger	F	feed
ε	exergy efficiency	hs	heat source	P	product
P	pressure	L	liter	0	standard condition
s	specific entropy, kJ/kg-k	COP	Coefficient of Performance	Se	separator
T	temperature	TPD	Tone Per Day	Vap	vapor
$\dot{W}$	power consumption rate, kW	SEC	Specific Energy Consumption	Liq	liquid
$\dot{Q}$	heat flow, kw	O&M	Operation and maintenance	i	i^{th} stage
		MR	Multi component refrigerant	n	n^{th} stage

References

[1] Y. E. Yuksel, M. Ozturk, and I. Dincer, “Analysis and assessment of a novel hydrogen liquefaction process,” International journal of hydrogen energy, vol. 42, no. 16, pp. 11429-11438, 2017.

[2] B. Wang, X. Zhang, H.Bai, Y. Lü, S. Hu, Hydrogen production from methanol through dielectric barrier discharge, Frontiers of Chemical Science and Engineering, 5(2), 209-214, 2011.

[3] D. O. Berstad, J. H. Stang, and P. Nekså, “Comparison criteria for large-scale hydrogen liquefaction processes,” International Journal of Hydrogen Energy, vol. 34, no. 3, pp. 1560-1568, 2009.

[4] F. Etternavn, “Efficient Hydrogen Liquefaction Processes,” University of Science and Technology, 2013.

[5] T. Riis, E.F. Hagen, P.J. Vie, Q. Ulleberg, Hydrogen production and storage—R&D priorities and gaps. International Energy Agency-Hydrogen Co-Ordination Group-Hydrogen Implementing Agreement. 2006.

[6] J. Wisniak, Louis Paul Cailletet—The liquefaction of the permanent gases. 2003.

[7] S. Krasae-in, J. H. Stang, and P. Neksa, “Development of large-scale hydrogen liquefaction processes from 1898 to 2009,” International Journal of Hydrogen Energy, vol. 35, no. 10, pp. 4524-4533, 2010.

[8] C. Baker, and R. Shaner, “A study of the efficiency of hydrogen liquefaction,” International Journal of Hydrogen Energy, vol. 3, no. 3, pp. 321-334, 1978.

[9] H. Matsuda, and M. Nagami, “Study of large hydrogen liquefaction process,” 수소에너지, vol. 8, no. 3, pp. 175-175, 1997.

[10] H. Quack, "Conceptual design of a high-efficiency large capacity hydrogen liquefier, AIP Conference Proceedings. Vol. 613. No. 1. American Institute of Physics, 2002.

[11] W. L. Staats, "Analysis of a supercritical hydrogen liquefaction cycle," Ph.D. Thesis, Massachusetts Institute of Technology, 2008.
[12] G. Valenti, and E. Macchi, "Proposal of an innovative, high-efficiency, large-scale hydrogen liquefier," International Journal of Hydrogen Energy, vol. 33, no. 12, pp. 3116-3121, 2008.
[13] D. O. Berstad, J. H. Stang, and P. Nekså, "Large-scale hydrogen liquefier utilising mixed-refrigerant pre-cooling," International Journal of Hydrogen Energy, vol. 35, no. 10, pp. 4512-4523, 2010.
[14] S. Krasae-In, J. H. Stang, and P. Neksa, "Simulation on a proposed large-scale liquid hydrogen plant using a multi-component refrigerant refrigeration system," International journal of hydrogen energy, vol. 35, no. 22, pp. 12531-12544, 2010.
[15] G. Valenti, E. Macchi, and S. Brioschi, "The influence of the thermodynamic model of equilibrium-hydrogen on the simulation of its liquefaction," International journal of hydrogen energy, vol. 37, no. 14, pp. 10779-10788, 2012.
[16] H. T. Walnum, D. Berstad, M. Drescher, P. Neksa, H. Quack, C. Haberstroh, J. Essler, Principles for the liquefaction of hydrogen with emphasis on precooling processes. 12th Cryogenics 2012-IIR Conference, 2012.
[17] S. Krasae-in, "Optimal operation of a large-scale liquid hydrogen plant utilizing mixed fluid refrigeration system," International journal of hydrogen energy, vol. 39, no. 13, pp. 7015-7029, 2014.
[18] H. Quack, C. Haberstroh, I. Seemann et al., "Nelium, a Refrigerant with High Potential for the Temperature Range between 27 and 70 K," Physics Procedia, vol. 67, pp. 176-182, 2015.
[19] M. Asadnia, and M. Mehrpooya, "A novel hydrogen liquefaction process configuration with combined mixed refrigerant systems," International journal of hydrogen energy, vol. 42, no. 23, pp. 15564-15585, 2017.
[20] M. S. Sadaghiani, M. Mehrpooya, and H. Ansarinasab, "Process development and exergy cost sensitivity analysis of a novel hydrogen liquefaction process," International journal of hydrogen energy, vol. 42, no. 50, pp. 29797-29819, 2017.
[21] U. Cardella, L. Decker, J. Sundberg, H. Klein, Process optimization for large-scale hydrogen liquefaction. International Journal of Hydrogen Energy, 42:12339-54, 2017.
[22] L. Yin, and Y. Ju, "Process optimization and analysis of a novel hydrogen liquefaction cycle," International Journal of Refrigeration, vol. 110, pp. 219-230, 2020.
[23] G. J. Kramer, J. Huijsmans, and D. Austgen, "Clean and green hydrogen." 16th World hydrogen energy conference. Vol. 16. 2006
[24] A. Kuendig, K. Loehlein, G. Kramer et al., "Large scale hydrogen liquefaction in combination with LNG regasification, Proceedings of the 16th world hydrogen energy conference, pp. 3326-3333, 2006.
[25] J.-H. Yang, Y. Yoon, M. Ryu et al., "Integrated hydrogen liquefaction process with steam methane reforming by using liquefied natural gas cooling system," Applied Energy, vol. 255, pp. 113840, 2019.
[26] M. Mehrpooya, M. S. Sadaghiani, and N. Hedayat, "A novel integrated hydrogen and natural gas liquefaction process using two multistage mixed refrigerant refrigeration systems," International journal of energy research, vol. 44, no. 3, pp. 1636-1653, 2020.
[27] H.-M. Chang, B. H. Kim, and B. Choi, "Hydrogen liquefaction process with Brayton refrigeration cycle to utilize the cold energy of LNG," Cryogenics, vol. 108, pp. 103093, 2020.
[28] V. Belyakov, B. Krakovskii, O. Popov et al., "Low-capacity hydrogen liquefier with a helium cycle," Chemical and Petroleum Engineering, vol. 38, no. 3, pp. 150-153, 2002.
[29] A.V. Zhuzhgov, O. Krivoruchko, L. Isupova, O. Mart'yanov, V. Parmon, Low-Temperature Conversion of ortho-Hydrogen into Liquid para-Hydrogen: Process and Catalysts. Review. Catalysis in Industry, 10:9-19, 2018.
[30] G. Skaugen, D. Berstad, Ø. Wilhelmsen, Comparing exergy losses and evaluating the potential of catalyst-filled plate-fin and spiral-wound heat exchangers in a large-scale Claude hydrogen liquefaction process. International journal of hydrogen energy, 45:6663-79, 2020.
[31] A. Hammad, I. Dincer, Analysis and assessment of an advanced hydrogen liquefaction system. International journal of hydrogen energy, 43:1139-51, 2018.
[32] H. Ansarinasab, M. Mehrpooya, A. Mohammadi, Advanced exergy and exergoeconomic analyses of a hydrogen liquefaction plant equipped with mixed refrigerant system. Journal of cleaner production. 144:248-59, 2017.
[33] H. Ansarinasab, M. Mehrpooya, M. Sadeghzadeh, An exergy-based investigation on hydrogen liquefaction plant-exergy, exergoeconomic, and exergoenvironmental analyses. Journal of cleaner production, 210:530-41, 2019.
[34] I. Kuz'menko, I. Morkovkin, and E. Gurov, "Concept of building medium-capacity hydrogen liquefiers with helium refrigeration cycle," Chemical and Petroleum Engineering, vol. 40, no. 1, pp. 94-98, 2004.
[35] K. Ohlig, L. Decker, The latest developments and outlook for hydrogen liquefaction technology. ADVANCES IN CRYOGENIC ENGINEERING: Transactions of the Cryogenic Engineering Conference-CEC: AIP Publishing, p. 1311-7, 2014.
[36] J. Kumar, S. Nair, R. Menon, M. Goyal, N. Ansari, A. Chakravarty, V. Joemon, Helium refrigeration system for hydrogen liquefaction applications. IOP Conference Series: Materials Science and Engineering: IOP Publishing, Vol. 171, No. 1, p. 012029, 2017.

[37] H.-M. Chang, K. N. Ryu, and J. H. Baik, "Thermodynamic design of hydrogen liquefaction systems with helium or neon Brayton refrigerator," Cryogenics, vol. 91, pp. 68-76, 2018.
[38] J. Stang, P. Neksa, and E. Brendeng, "On the design of an efficient hydrogen liquefaction process," 2006.
[39] Shimko M, Gardiner M. Innovative hydrogen liquefaction cycle. 2008.
[40] S. Krasae-In, J. Stang, P. Neksa, Exergy analysis on the simulation of a small-scale hydrogen liquefaction test rig with a multi-component refrigerant refrigeration system. International journal of hydrogen energy, 35:8030-42, 2010.
[41] S. Krasae-in, A. M. Bredesen, J. Stang, P. Neksa, Simulation and experiment of a hydrogen liquefaction test rig using a multi-component refrigerant refrigeration system. International journal of hydrogen energy, 36:907-19, 2011.
[42] M. Aasadnia, and M. Mehrpooya, "Large-scale liquid hydrogen production methods and approaches: A review," Applied Energy, vol. 212, pp. 57-83, 2018.
[43] T. A. H. Ratlamwala, I. Dincer, M. Gadalla, M. Kanoglu, Thermodynamic analysis of a new renewable energy based hybrid system for hydrogen liquefaction. International Journal of Hydrogen Energy, 37:18108-17, 2012.
[44] C. Yilmaz, M. Kanoglu, A. Bolatturk, M. Gadalla, Economics of hydrogen production and liquefaction by geothermal energy. International journal of hydrogen energy, 37:2058-69, 2012.
[45] M. Aasadnia, and M. Mehrpooya, "Conceptual design and analysis of a novel process for hydrogen liquefaction assisted by absorption precooling system," Journal of cleaner production, vol. 205, pp. 565-588, 2018.
[46] B. Ghorbani, M. Mehrpooya, M. Aasadnia et al., "Hydrogen liquefaction process using solar energy and organic Rankine cycle power system," Journal of cleaner production, 2019.
[47] M. Aasadnia, M. Mehrpooya, and H. Ansarinasab, "A 3E evaluation on the interaction between environmental impacts and costs in a hydrogen liquefier combined with absorption refrigeration systems," Applied Thermal Engineering, pp. 113798, 2019.
[48] Ö. Kaşka, C. Yılmaz, O. Bor et al., "The performance assessment of a combined organic Rankine-vapor compression refrigeration cycle aided hydrogen liquefaction," International Journal of Hydrogen Energy, vol. 43, no. 44, pp. 20192-20202, 2018.
[49] C. Yilmaz, and O. Kaska, "Performance analysis and optimization of a hydrogen liquefaction system assisted by geothermal absorption precooling refrigeration cycle," International Journal of Hydrogen Energy, vol. 43, no. 44, pp. 20203-20213, 2018.
[50] T. Parikhani, T. Gholizadeh, H. Ghaebi, S. M. S. Sadat, M. Sarabi, Exergoeconomic optimization of a novel multigeneration system driven by geothermal heat source and liquefied natural gas cold energy recovery. Journal of cleaner production, 209:550-71, 2019.
[51] C. Yilmaz, A case study: exergoeconomic analysis and genetic algorithm optimization of performance of a hydrogen liquefaction cycle assisted by geothermal absorption precooling cycle. Renewable Energy, 128:68-80, 2018.
[52] S. Seyam, I. Dincer, M. Agelin-Chaab, Analysis of a clean hydrogen liquefaction plant integrated with a geothermal system. Journal of cleaner production, 243:118562, 2020.
[53] M. Nouri, M. Miansari, B. Ghorbani, Exergy and economic analyses of a novel hybrid structure for simultaneous production of liquid hydrogen and carbon dioxide using photovoltaic and electrolyzer systems, Journal of cleaner production, 120862, 2020.
[54] J. E. Bae, S. Wilailak, J. H. Yang, D. Y. Yun, U. Zahid, C. J. Lee, Multi-objective optimization of hydrogen liquefaction process integrated with liquefied natural gas system, Energy Conversion and Management, 231:113835, 2021.
[55] B. Ghorbani, A. Ebrahimi, S. Rooholamini, M. Ziabasharhagh, Integrated Fischer-Tropsch synthesis process with hydrogen liquefaction cycle. Journal of cleaner production, 283:124592, 2021.
[56] M. S. Sadaghiani, and M. Mehrpooya, "Introducing and energy analysis of a novel cryogenic hydrogen liquefaction process configuration," International journal of hydrogen energy, vol. 42, no. 9, pp. 6033-6050, 2017.
[57] H. Rezaie Azizabadi, M. Ziabasharhagh, M. Mafi, Introducing a proper hydrogen liquefaction concept for using wasted heat of thermal power plants-case study: Parand gas power plant. Chinese Journal of Chemical Engineering. 2021.
[58] D. Berstad, G. Skaugen, Ø. Wilhelmsen, Dissecting the exergy balance of a hydrogen liquefier: Analysis of a scaled-up claude hydrogen liquefier with mixed refrigerant pre-cooling. International journal of hydrogen energy, 46:8014-29, 2021.
[59] M. Bracha, G. Lorenz, A. Patzelt et al., "Large-scale hydrogen liquefaction in Germany," International Journal of Hydrogen Energy, vol. 19, no. 1, pp. 53-59, 1994.
[60] S. S. Chadwick, "Ullmann's Encyclopedia of Industrial Chemistry," Reference Services Review, vol. 16, no. 4, pp. 31-34, 1988.
[61] H. W. Woolley, R. B. Scott, and F. Brickwedde, Compilation of thermal properties of hydrogen in its various isotopic and ortho-para modifications: Citeseer, 1948.
[62] G. Reuss, W. Disteldorf, O. Grundler et al., "Ullmann's Encyclopedia of Industrial Chemistry, vol. A11," Wiley-VCH, Weinheim, 2008.
[63] N. T. Stetson, R. C. Bowman Jr, G. L. Olson, Overview of hydrogen storage, transportation, handling and distribution. Handbook of

Hydrogen Energy, 586-611, 2014.
[64] E85. A. Ebrahimi, B. Ghorbani, and M. Ziabasharhagh, "Pinch and sensitivity analyses of hydrogen liquefaction process in a hybridized system of biomass gasification plant, and cryogenic air separation cycle," Journal of cleaner production, vol. 258, pp. 120548, 2020.
[65] H. Rezaie Azizabadi, M. Ziabasharhagh, M. Mafi, Applicability of the common equations of state for modeling hydrogen liquefaction processes in Aspen HYSYS. Gas Processing Journal, 9:11-28, 2020.
[66] R.F. Barron, Cryogenic systems. Monographs on cryogenics, 1985.
[67] M. Mehrpooya, M. Hossieni, and A. Vatani, "Novel LNG-based integrated process configuration alternatives for coproduction of LNG and NGL," Industrial & engineering chemistry research, vol. 53, no. 45, pp. 17705-17721, 2014.
[68] B. Ghorbani, G. Salehi, H. Ghaemmaleki et al., "Simulation and optimization of refrigeration cycle in NGL recovery plants with exergy-pinch analysis," Journal of Natural Gas Science and Engineering, vol. 7, pp. 35-43, 2012.
[69] S. Aprhornratana, and I. Eames, "Thermodynamic analysis of absorption refrigeration cycles using the second law of thermodynamics method," International Journal of Refrigeration, vol. 18, no. 4, pp. 244-252, 1995.
[70] B. R. Bakshi, T. G. Gutowski, and D. P. Sekulić, Thermodynamics and the Destruction of Resources: Cambridge University Press, 2011.
[71] T. J. Kotas, The exergy method of thermal plant analysis, Elsevier, 2013.